

Superconductivity-induced magnetoresistance suppression in hybrid superconductor/magnetic tunnel junctions

Yin-Ming Chang and Kai-Shin Li

Department of Physics, National Taiwan University, 106 Taipei, Taiwan

Wen-Chung Chiang*

Department of Physics, Chinese Culture University, 111 Taipei, Taiwan

Jiunn-Yuan Lin[†]

Department of Physics, National Chiao Tung University, 300 Hsinchu, Taiwan

Minn-Tsong Lin[‡]

Department of Physics, National Taiwan University, 106 Taipei, Taiwan

and Institute of Atomic and Molecular Sciences, Academia Sinica, 106 Taipei, Taiwan

(Received 15 August 2008; revised manuscript received 13 November 2008; published 12 January 2009)

Hybrid superconductor/magnetic tunnel junctions of Nb/CoFe/AlO/CoFe/NiFe have been implemented to investigate the impact of the superconducting Nb layer on the proximal ferromagnetic CoFe layer. A suppression of tunneling magnetoresistance effect is observed as the Nb layer undergoes the superconducting transition. This suppression is thought to be due primarily to the coupling of the magnetic inhomogeneity of CoFe to the superconductivity of Nb. The magnetic structure-vortex interactions interplay each other, inducing a complex domain evolution in the magnetization process and consequently degrading the junction's antiparallel magnetization alignment.

DOI: [10.1103/PhysRevB.79.012401](https://doi.org/10.1103/PhysRevB.79.012401)

PACS number(s): 85.75.-d, 75.47.-m, 74.90.+n, 73.40.Gk

The interplay between the antagonistic orderings of ferromagnetism and superconductivity has introduced many novel effects in both science and technology. For example, one might expect that ferromagnetism overwhelms the superconducting orderings on the scale of the exchange length when the two types of materials are brought next to each other. Nevertheless, several experimental results have evidenced that the mutual influence between the superconductor and the ferromagnet extends much longer.^{1,2} Application-wise, the vortex pinning in the superconductor/ferromagnet (S/F) hybrid is found to efficiently enhance the critical current.³ In addition, the artificial structure of ferromagnet/superconductor/ferromagnet (F/S/F) has been proposed as a spin-valve device for supercurrent.⁴ All these have suggested that the heterostructural combination of superconductor and ferromagnet could potentially enhance the functionality of individual materials.

Analogous to the stacking of the supercurrent spin valves, a magnetic tunnel junction (MTJ) is comprised of ferromagnet/insulator/ferromagnet (F/I/F) trilayers. The fact that the junction's resistance changes drastically with the relative orientation of the ferromagnets makes MTJ advanta-

geous in applications for magnetic sensor and nonvolatile memory devices. The tunneling magnetoresistance (TMR) ratio, defined as the percentage change of the junction's resistance (from antiparallel to parallel magnetization), is commonly used as an indication for the junction's performance. In this Brief Report, we report the experiments of placing a superconducting Nb layer adjacent to the ferromagnetic layer in a MTJ structure. The composite S/F electrodes have been used widely in the current-perpendicular-to-plane (CPP) measurements to enhance the junction's current uniformity.⁵ Nevertheless, due to the sensitivity of TMR, the induced magnetic excitation by superconductivity could result directly in the junction's resistance change. Thus the superconductor/magnetic tunneling junction (S/MTJ) hybrid provides a unique system for studying the interplay between superconductivity and ferromagnetism. Our results show a suppression of the TMR ratio as the adjacent Nb layer becomes superconducting. The fact that superconductivity impacts on the junction's resistance is crucial for future MTJ applications.

The layer sequence of our hybrid S/MTJs is

$$\text{Nb}(t_{\text{Nb}}, \text{ in nm})/\text{Co}_{0.75}\text{Fe}_{0.25}(30)/\text{Al}_2\text{O}_3(2.5)/\text{Co}_{0.75}\text{Fe}_{0.25}(15)/\text{Ni}_{0.8}\text{Fe}_{0.2}(10)$$

with varying Nb layer thicknesses t_{Nb} . The whole stack was prepared in a magnetron sputtering system having a base pressure of 5×10^{-8} torr. All metallic layers were made with an Ar working pressure of 5×10^{-3} torr whereas the tunneling barrier was made by bathing a thin Al layer in an oxygen

plasma of 3×10^{-2} torr for 5 min. In order to perform the CPP four contact measurements, the junctions were patterned into cross stripes with the linewidth of 150 μm . The junction area is therefore defined by their intersection. The room-temperature TMR ratio of the junctions is typically around

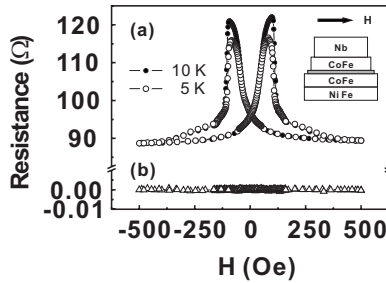


FIG. 1. (a) The magnetoresistance curves for the hybrid S/MTJ sample with $t_{\text{Nb}}=240$ nm, measured at 10 K (solid circle) and 5 K (open circle), respectively. Inset: the junction's structural profile and the corresponding field orientation. (b) The resistance curve for the Nb overlayer at 5 K.

25% with the tunneling resistivity in the range of $1-10 \text{ M}\Omega \mu\text{m}^2$. Layers were patterned with subsequent shadow masks without breaking the vacuum in order to keep the interfaces intact as many previous studies have indicated that the performance of a MTJ degrades significantly in the presence of interfacial imperfections.^{6,7} The CPP four contact resistance measurements were carried out in a physical properties measurement system (PPMS) where the resistances of the Nb layer itself and the entire junction were taken simultaneously using separate channels. The superconducting transition temperature T_c of Nb is determined by the midpoint of the transition.

Figure 1(a) shows the magnetoresistance (MR) curves for the junction with $t_{\text{Nb}}=240$ nm, measured at $T=10$ K (solid symbols, above the Nb T_c) and $T=5$ K (open symbols, below the Nb T_c), respectively. The field orientation with respect to the junction and the junction's structural profile are also demonstrated. The saturated resistances are nearly identical for the two curves, whereas the maximum resistance (obtained at a field around 95 Oe) drops noticeably as the temperature is reduced from 10 to 5 K. It is generally the case that as temperature decreases, the junction's resistance increases due to the suppression of the thermally assisted transport process. The TMR ratio also increases as the spin polarization of the tunneling current rises.⁸ The contradictory results shown in Fig. 1(a) indicate a strong influence of the superconductor upon the proximal ferromagnet. The measurement of the Nb resistance, as indicated in Fig. 1(b), ensures the presence of superconductivity during the field sweeping at $T=5$ K.

The TMR ratio of the same S/MTJ sample is plotted as a function of temperature in Fig. 2. An inset is included to show the resistance change of the Nb layer with $T_c=9.16$ K. The TMR ratio exhibits a sharp decrease as the temperature is reduced from 9 to 7 K, consistent with the onset of the superconducting transition, but the decrease is nonmonotonic. As temperature is further reduced, a local maximum is observed at $T=4$ K, followed by another downturn when the temperature is reduced toward 2 K. Similar nonmonotonic behavior is also seen in the other S/MTJ samples of our preparation.

It is known that not only temperature and magnetic field but also the layer thickness of the superconductor itself is related to the strength of the superconducting ordering. Fig.

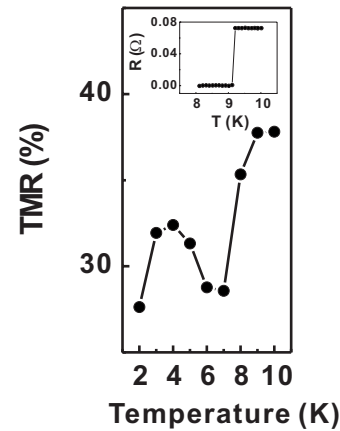


FIG. 2. The plot of TMR ratio with respect to temperature for the S/MTJ sample with $t_{\text{Nb}}=240$ nm. Inset indicates the resistance variation of the Nb overlayer in the neighborhood of the superconducting phase transition ($T_c=9.16$ K).

ure 3 shows the normalized TMR ratio as a function of temperature for a series of six hybrid S/MTJs with t_{Nb} ranging from 80 to 240 nm. The TMR ratio is normalized to unity at $T=10$ K and each curve is offset from the other by a scale of 0.1 for ease of comparison. The superconducting transition temperature for each sample is indicated by an arrow at the corresponding curve. Similar to the sample with $t_{\text{Nb}}=240$ nm, a significant suppression of the TMR ratio is also observed in the other samples when Nb becomes superconducting. The suppression is the greatest for the sample with the largest t_{Nb} (down by a factor of 0.27), but it is not completely clear whether all samples have reached their maximum TMR suppression due to the nonmonotonic changes. Nevertheless, during the cooling process, the TMR ratio never regains the level before the onset of the superconducting transition even a local maximum is present in the nonmonotonic variation.

The complex feature of the curves exhibited in Fig. 3 leads naturally to the concern of the magnetization process mechanism. Many factors are known to play influential roles in the magnetic reversal process, and hence the tunneling behavior. Such factors include the field history, the cooling process, the geometry and the uniformity of the ferromagnetic layers, etc. One might tend to exclude the influence of the superconductor on the interface electronic structure, as suggested in Fig. 1(a), by the fact that there is no significant difference between the saturated resistances above and below T_c . But such a possibility cannot simply be ruled out because the strength of the superconducting ordering depends not only on temperature, but also on the applied magnetic field.

In order to clarify this point, we further examine the correlation between the magnetization process and the temperature dependence of the junction's tunneling resistance by performing the following measurements on the sample with $t_{\text{Nb}}=140$ nm. First we set the temperature at $T=15$ K, sweeping the field until the maximum resistance is reached (at 122 Oe). Then the sample is held at this field, with temperature being swept from 15 to 2 K and back to 15 K. The results of the temperature sweeping for both directions are identical. A similar procedure is performed at an initial tem-

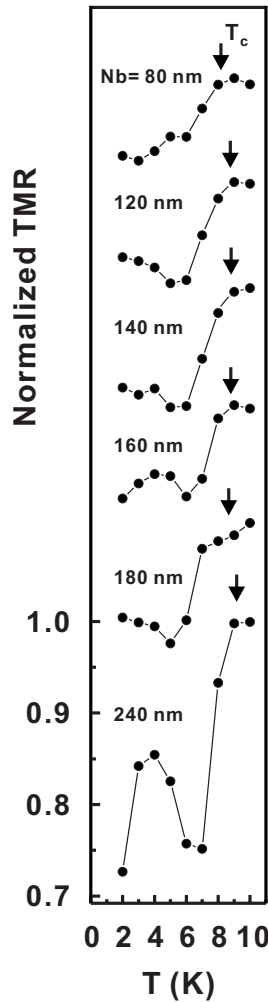


FIG. 3. Tunneling magnetoresistance versus temperature for a series of S/MTJ samples with t_{Nb} ranging from 80 to 240 nm. The TMR ratio is normalized to the value at 10 K. Each curve is offset by a scale of 0.1 for ease of comparison and is indicated by an arrow for the corresponding superconducting transition temperature.

perature of 2 K (the maximum resistance is reached also at 122 Oe), while the temperature sweeping is reversed (from 2 to 15 K). The two sweeping curves are shown in Fig. 4. The first curve (open circle), with an initial temperature $T = 15$ K, has an overall higher resistance value than the second curve (solid square, initial temperature $T = 2$ K). The two curves remain relatively level and smooth. If the previously observed suppression of TMR resulted from the electronic structure change of the ferromagnetic CoFe layer, one would anticipate the curves in Fig. 4 to exhibit a significant change in the neighborhood of the superconducting transition. We observe no such effect in our experiments. The inset of Fig. 4 magnifies the scales of the first curve near T_c . The small bumps shown in the inset are possibly caused by the disturbance of the stray field around domain structures as a result of Meissner screening, as reported elsewhere.⁹

The lower overall resistance value of the second curve in Fig. 4 reveals the fact that once the magnetization process of a S/MTJ sample is initiated at a temperature below T_c , the

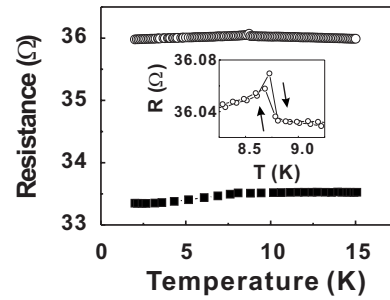


FIG. 4. Measurements of the junction's ($t_{\text{Nb}} = 140$ nm) peak resistance versus temperature. The first measurement (open circle) is initiated at 15 K, whereas the second (solid square) is initiated at 2 K. The corresponding peak resistance is achieved at the initial temperature, and during the subsequent temperature sweeping, the field is held still at 122 Oe (please see the text content for details). Inset magnifies the scales of the first curve near T_c whereas the arrows illustrate the temperature sweeping.

perfect antiparallel state can never be achieved. But when the “perfect” antiparallel magnetization state is obtained at a higher-than- T_c temperature, the ferromagnetic anisotropy seems to prevail over the influence of superconductivity. Thus the suppression of TMR is more likely to be caused by the superconductivity-induced domain evolution during the magnetization process in which the superconductor impedes the ferromagnet's magnetization reversal and effectively degrades the antiparallel alignment of the ferromagnets.

Researchers have found in either in-plane or perpendicular magnetization that vortex pinning could result from the intrinsic magnetic inhomogeneity or through artificial magnetic arrays.^{3,10–12} Interesting results were demonstrated by Van Bael *et al.*¹⁰ in a thin superconducting Pb film covering single-domain Co dots where flux lines were pinned at specific poles of the dipoles due to the interaction with the vortexlike structures. A simple question arises immediately from the viewpoint of fundamental physics: does the counter-effect, that is, the flux dynamics of superconductors, also influence the magnetic domain motion? In the present work, the nature of the effect has first been probed and observed in a hybrid S/MTJ system. Our experimental results show that upon the onset of superconducting transition, the TMR ratio drops significantly, indicating the immediate spin structure change as induced by the superconducting vortex dynamics. The detailed mechanism can thus be described as the following: when the magnetization process of a S/MTJ is initiated in the presence of superconductivity, the homogeneity of the adjacent ferromagnet can no longer persist as the sample is set toward the demagnetization state. The interplay between the domain-vortex interactions steps in and the interactions are strongly coupled. The magnetic domain structures then evolve in a more complex way (as compared to the situation when no superconductivity is present). The key issue lies in the fact that there are two important interfaces involved, i.e., the ferromagnet F/I and the S/F interfaces. The former is considered mostly responsible for the rise of TMR and it exhibits a sharp response to the events happening on the S/F side through the change in magnetoresistance. Therefore the hybrid S/MTJ does provide a unique and sensitive system to probe the S-F interplay.

The complexity of domain evolution has manifested itself by the noncommutable effects of temperature and magnetic field illustrated in Fig. 4, and the nonmonotonic MR change in the cooling process below T_c is also a reflection of that (Figs. 2 and 3). As temperature is further reduced, the domain structures rearrange themselves toward a metastable state which associates with relatively more moments aligning in an antiparallel situation, causing the MR to rise again. By referring to such metastable states with regard to the temperature variation, the oscillatory behavior therefore indicates the instability of the antiparallel alignment as the domains are still under the strong influence of the vortex dynamics. The parallel magnetization state, on the other hand, is unaffected regardless of the presence of superconductivity since the coupling is overwhelmed by the applied magnetic field.

In conclusion, a series of hybrid superconductor/magnetic tunnel junctions has been used to investigate the interplay between superconductivity and ferromagnetism. The result-

ing tunneling magnetoresistance shows a significant suppression in the presence of superconductivity and the change is nonmonotonic in the cooling process below T_c . This indicates the existing nature of superconductivity-ferromagnetism interaction—that superconducting vortices interact with magnetic domains, causing their complex evolution, degrading the junction's antiparallel magnetization alignment, and therefore suppressing the tunneling magnetoresistance. The results are valuable not only from the viewpoint of fundamental physics, but also from that of device applications, especially when the composite of superconducting and ferromagnetic materials is involved.

This work was supported in part by the National Science Council of Taiwan through Grants No. NSC 95-2112-M-002-051-MY3 and No. NSC 96-2120-M-002-011. Acknowledgments are given to W. J. Chang, S. S. Chang, L. W. Kuo, and B. C. Lin for their technical support.

*wchiang@faculty.pccu.edu.tw

†ago@cc.nctu.edu.tw

‡Author to whom correspondence should be addressed; mtlin@phys.ntu.edu.tw

¹V. T. Petrashov, I. A. Sosnin, I. Cox, A. Parsons, and C. Troadec, *Phys. Rev. Lett.* **83**, 3281 (1999).

²D. Stamopoulos, N. Moutis, M. Pissas, and D. Niarchos, *Phys. Rev. B* **72**, 212514 (2005).

³M. J. Van Bael, M. Lange, S. Raedts, V. V. Moshchalkov, A. N. Grigorenko, and S. J. Bending, *Phys. Rev. B* **68**, 014509 (2003).

⁴Ion C. Moraru, W. P. Pratt, Jr., and Norman O. Birge, *Phys. Rev. Lett.* **96**, 037004 (2006).

⁵J. M. Slaughter, W. P. Pratt, Jr., and P. A. Schroeder, *Rev. Sci. Instrum.* **60**, 127 (1989).

⁶C. H. Ho, Minn-Tsong Lin, Y. D. Yao, S. F. Lee, C. C. Liao, F. R.

Chen, and J. J. Kai, *J. Appl. Phys.* **90**, 6222 (2001).

⁷Minn-Tsong Lin, C. H. Ho, Y. D. Yao, R. T. Huang, C. C. Liao, F. R. Chen, and J. J. Kai, *J. Appl. Phys.* **91**, 7475 (2002).

⁸Yu Lu, X. W. Li, Gang Xiao, R. A. Altman, W. J. Gallagher, A. Marley, K. Roche, and S. Parkin, *J. Appl. Phys.* **83**, 6515 (1998).

⁹S. V. Dubonos, A. K. Geim, K. S. Novoselov, and I. V. Grigorieva, *Phys. Rev. B* **65**, 220513(R) (2002).

¹⁰M. J. Van Bael, J. Bekaert, K. Temst, L. Van Look, V. V. Moshchalkov, Y. Bruynseraede, G. D. Howells, A. N. Grigorenko, S. J. Bending, and G. Borghs, *Phys. Rev. Lett.* **86**, 155 (2001).

¹¹X. X. Zhang, G. H. Wen, R. K. Zheng, G. C. Xiong, and G. J. Lian, *Europhys. Lett.* **56**, 119 (2001).

¹²W. Gillijns, A. Yu. Aladyshkin, M. Lange, M. J. Van Bael, and V. V. Moshchalkov, *Phys. Rev. Lett.* **95**, 227003 (2005).